Catalysis Today 228 (2014) 212–218

Contents lists available at ScienceDirect

Catalysis Today

journal homepage: www.elsevier.com/locate/cattod

Oxidative coupling of methane—A complex surface/gas phase mechanism with strong impact on the reaction engineering

Benjamin Beck[a], Vinzenz Fleischer[a], Sebastian Arndt[a], Miguel González Hevia[b], Atsushi Urakawa[b], Peter Hugo[a], Reinhard Schomäcker[a,*]

[a] Technische Universität Berlin, Institut für Chemie, Straße des 17. Juni 124, 10623 Berlin, Germany
[b] Institute of Chemical Research of Catalonia, Avgda. Països Catalans 16, 43007 Tarragona, Spain

ARTICLE INFO

Article history:
Received 13 July 2013
Received in revised form
14 November 2013
Accepted 23 November 2013
Available online 9 January 2014

Keywords:
$Mn/Na_2WO_4/SiO_2$
Oxidative coupling of methane
High pressure
Temporal analysis of products
Maximum yield

ABSTRACT

The oxidative coupling of methane over $Mn/Na_2WO_4/SiO_2$ has been investigated at reaction conditions suitable for industrial applications up to 10 bar in a fixed bed reactor as well as by temporal analysis of products (TAP) by admitting pulses of methane, ethane and ethene oxygen mixtures. The influence of pressure on selectivity is investigated and a concept for optimizing it is derived. A maximum yield is estimated from the ratios of the involved main reactions of the reaction network assuming that the undesired parallel reactions can be suppressed.

1. Introduction

Oxidative coupling of methane (OCM) to ethylene offers great industrial potential, because it would broaden the feedstock basis for chemical industry. Today crude oil derived olefins and aromatic hydrocarbons via steam cracking of naphtha are still the crucial raw materials for the majority of value added chains in chemical industry. The importance of alternative carbon sources for chemical processes becomes greater as oil price increases [1].

For the development of an OCM process $Mn/Na_2WO_4/SiO_2$ has been highlighted as catalyst from the rich literature on OCM [2,3], but little is known about its structure and the reaction mechanism at this catalyst. Its reported stability and high yield were the important motivations to select the catalyst for detailed studies [4–6]. However, the obtained yield still needs to be improved for industrial application.

In most reports the focus is mainly directed to the catalyst material, and reactor setups and conditions are designed and selected in a way that no reaction of methane is observed in an empty reactor. One has to mention that for industrial application high pressures are necessary to make the process economically viable, but detailed studies of empty reactors at higher pressures are missing in literature. Furthermore, the consecutive reactions of the targeted C_2 products has the strongest negative impact on the yield [7–9]. Reactivity data of ethane or ethylene at increased pressures are almost not existent in the literature. At typical OCM conditions of 800 °C virtually no material typically used for these reactors or packing is absolutely chemically inert. For the development of an industrial scale reactor one should expect that these factors contribute even more to the reaction, due to use of materials like stainless steel. The purpose of this paper is to point out important factors which have to be considered for the reaction engineering of OCM including the interaction of gas phase and surface reactions.

The design of an industrial scale reactor requires knowledge about the reaction kinetics. If a reaction network shares strong contributions of gas phase and surface reactions, it is very difficult to derive this knowledge from experimental series at typical reaction conditions with the use of a fixed bed reactor only. This is due to inseparable kinetic data of gas phase and surface contribution. OCM is known to function in a very complex reaction network containing a variety of surface and gas phase reactions, which is depicted in a simplified scheme in Fig. 1. Obviously, the yield of ethane and ethylene is strongly dependent on the parallel and consecutive reactions to carbon oxides. Obtaining more information about the surface catalyzed activation of methane, ethane and ethene requires suppression of the gas phase activation of these components, which can be attained at the very low pressure such as the condition of temporal analysis of products (TAP) reactors.

---

* Corresponding author. Tel.: +49 30 31424973.
E-mail address: schomaecker@tu-berlin.de (R. Schomäcker).

0920-5861/$ – see front matter © 2013 Elsevier B.V. All rights reserved.
http://dx.doi.org/10.1016/j.cattod.2013.11.059

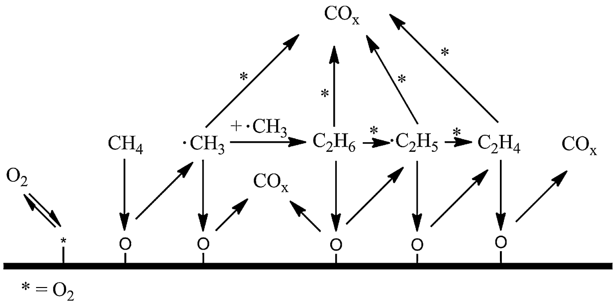

Fig. 1. Simplified reaction network of the oxidative coupling of methane at oxides.

2. Experimental

2.1. Catalyst synthesis

$Mn/Na_2WO_4/SiO_2$ catalyst material was prepared by fluidized bed processing of the constituent substances as described elsewhere [4]. The final catalyst contains 2 wt% Mn(II) and 5 wt% Na_2WO_4. A detailed characterization was also performed by Simon et al. [4].

2.2. Fixed bed reactor

OCM was investigated in a stainless steel reactor (65 cm length and 4 mm i.d.) equipped with an inlay made of corundum to minimize catalytic reactions at the reactor walls. This reactor can be operated up to 10 bars. The reaction temperature was between 700 and 800 °C. The product gases were analyzed with a gas chromatograph GC-2014 by Shimadzu, which was equipped with a methanizer and thermal conductivity and flame ionization detectors.

The reactor was filled with a fixed bed of quartz granules of 400 to 800 μm diameter up to height of 38 cm to end in the isothermal zone of the reactor. On the top of the quartz bed, a small piece of quartz wool was placed to keep the 100 mg $Mn/Na_2WO_4/SiO_2$ in position. The feeding mixture contained 95 vol% methane and 5 vol% oxygen with an overall gas flow rate between 50 to 500 N ml/min, in such a way that the residence time is kept constant with varying pressure. The shift of the explosion region to lower oxygen fractions with increasing pressure prohibits the usage of high oxygen fractions.

2.3. Temporal analysis of products

TAP experiments was conducted in a TAP-2 device, which is described in detail elsewhere [10]. In a small reactor (71 mm length and 4.6 mm i.d.) made of quartz, fixed bed 50 mg of catalyst (2–3 mm thickness) was placed, sandwiched by two layers of quartz particles. Both catalyst and quartz particles were in the 200–300 μm range. Before the TAP measurements the catalyst was pretreated for 30 min at 650 °C in oxygen flow. Measurements were performed at temperatures between 500 and 800 °C with pulse sizes large enough to be affected by intermolecular collisions (ca. 10^{17} molecules per pulse) due to the absence of desired products at small pulse sizes. Using the large pulse size, the mass transport is generally characterized as molecular diffusion regime.

Two types of experiments were conducted: simultaneous pulsing and sequential pulsing of oxygen and the specific hydrocarbon; i.e. methane, ethane or ethylene. The pulsed gas consisted of a hydrocarbon to oxygen to neon (internal standard) mixture of 2/1/4. In the case of sequential pulsing the methane to oxygen ratio cannot set accurately due the usage of two pulse valves and is adjusted individually to obtain accurate TAP responses. In the case of MgO a methane to oxygen ratio of roughly 6 to 1 is obtained. In the case of $Mn/Na_2WO_4/SiO_2$ the methane to oxygen ratio was roughly 1 to 1. The response pulses of each component were calculated by averaging ten pulses per investigated atom mass unit (amu). Since carbon monoxide, carbon dioxide, ethene and ethane share some relevant amus, it was necessary to use the fragmentation patterns of these compounds for quantification. For the sake of comparison, we have also investigated magnesia by TAP as reference beside $Mn/Na_2WO_4/SiO_2$. It is well known that doping magnesia with lithium results in an enhanced catalytic performance, but the instability of this system prevents a closer investigation by TAP experiments.

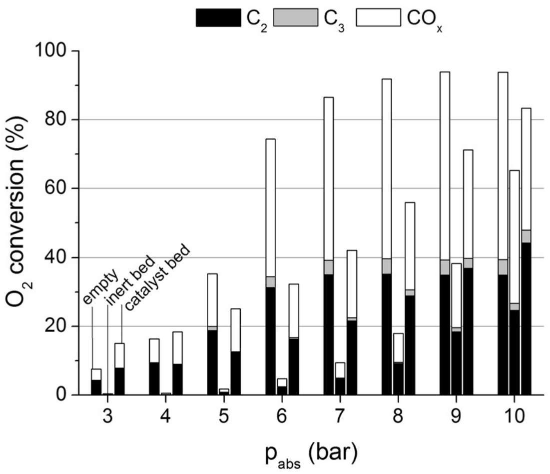

Fig. 2. Oxygen conversion with resulting product distribution at constant residence time at various pressures at 700 °C.

3. Results and discussion

3.1. Catalyst characterization

A detailed characterization of the used $Mn/Na_2WO_4/SiO_2$ is given by Simon et al. [4]. The catalyst support was homogenously coated with Na/WO_4 and Mn precursors resulting in crystalline phases of Mn_2O_3 and Na_2WO_4. The support is transformed into the stable cristobalite phase with a macroporous surface morphology. The final catalyst contains 2 wt% Mn(II) and 5 wt% Na_2WO_4 and has a surface area of 1.86 m^2/g. The catalyst was chemically and mechanically stable during OCM. Magnesium oxide was purchased from Sigma-Aldrich (99.9%) and has a surface area of 78 m^2/g.

3.2. Pressure experiments

The results of the OCM reaction at up to 10 bar and 700 °C are shown in Fig. 2. Experiments were performed with an empty reactor (left), a fix bed of quartz granules (middle) and a fixed bed of quartz granules with a layer of catalyst on top of it (right). The tint inside the columns specifies the yield to carbon oxides, C_2 and C_3 components, respectively. The carbon balance for the pressure experiments did not deviate more than 0.5%. Strikingly the empty reactor results in the highest conversion of oxygen over the full range of examined pressure, reaching almost complete conversion at 8 bar. Only a small increase in C_{2+} yield is observed above 5 bar, which is caused by the increasing influence of the total oxidation of the C_{2+} components. The sigmoid characteristic of the oxygen conversion is typical for reactions with orders higher than one. In contrast, the fixed bed of quartz granules results in a reduced residence time that leads to the lowest conversion over the complete range of pressure. The behavior seems to be almost the same as

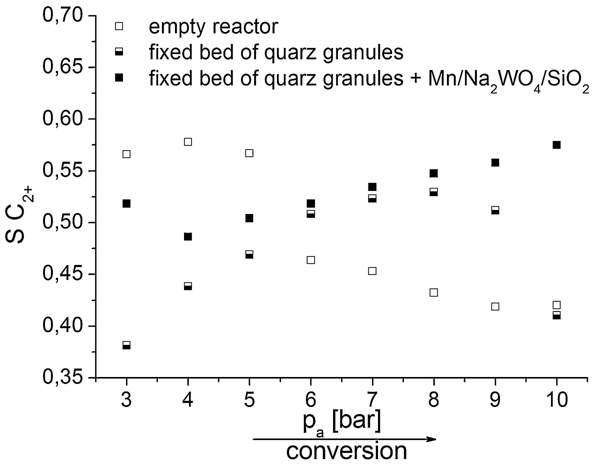

Fig. 3. Influence of absolute pressure on C_{2+} selectivity at constant residence time.

in the empty reactor with a shift to higher pressures. Addition of $Mn/Na_2WO_4/SiO_2$ on top of the quartz fixed bed regains higher oxygen conversions. The absence of a clear sigmoid behavior with increasing pressure indicates a more surface controlled reaction sequence, with a much higher yield of C_{2+} components compared to the reactor loaded only with quartz.

Fig. 3 shows the corresponding selectivities to C_{2+} at the investigated pressures. The empty reactor as well as the fixed bed of quartz granules passes through a maximum selectivity to C_{2+} at 4 and 8 bar, respectively. In contrast, the addition of $Mn/Na_2WO_4/SiO_2$ results in a steady increase of selectivity to C_{2+} with increasing pressure. Its maximum is not reached in the investigated range of pressure. The C_2 selectivity in OCM is strongly affected by consecutive reactions. This results generally in a loss of selectivity with increasing conversion due to total oxidation [11]. The observation of a higher selectivity in combination with a higher methane and oxygen conversion implies a clear benefit of higher pressure toward better C_2 selectivity.

For detailed understanding of the homogeneous gas phase as well as the heterogeneous surface catalyzed reactions, it is necessary to quantify their contributions to the overall product mixture in order to maximize the C_{2+} yield. Zanthoff and Baerns developed a kinetic model for the gas phase contribution including 33 species and 192 elementary steps, which describes the product distribution and conversion at the end of the reactor accurately as long as the reactor temperature is higher than 600 °C [12,13]. A recent investigation of the spatial compositional profile along a reactor has exhibited discrepancies with the simulated profiles with respect to conversion and composition [13]. Better consistency could be achieved by extension of the gas phase model to more species and reactions. Marin et al. [14] coupled a gas phase reaction model to a heterogeneous catalysis one. However, the gas phase part alone of this model does not explain the observed increase in C_{2+} selectivity with increasing pressure at low oxygen conversions with quartz granules packing (Figs. 2 and 3) [15].

Nevertheless, it is necessary to couple the gas phase model to a model describing heterogeneous surface reactions. At typical reaction conditions their kinetic data are obviously compromised by gas phase contributions. This unusual approach is necessary due to the high complexity of OCM. Therefore we employed the TAP technique with the aim to directly obtain kinetic data of the CH bond activation reaction based on the assumption of the reaction as the rate determining step. Gaining the surface reactivity of C_1 and C_2 without the influence of gas phase reactions is expected to reveal factors maximizing the yield of desired products while minimizing the formation of the undesired CO_x by-products.

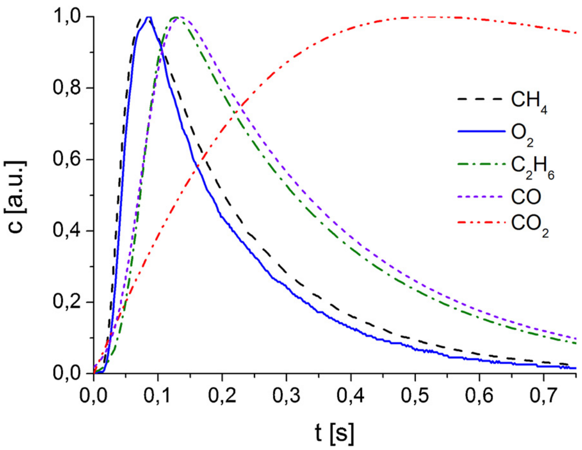

Fig. 4. TAP response of $CH_4/O_2/Ne$ (=4/1/2) pulse over magnesia at 700 °C.

3.3. *Temporal analysis of products*

Generally TAP measurements are performed with small pulse sizes resulting in gas transport by Knudsen diffusion, in which gas phase intermolecular collisions are negligible [16–19]. As depicted in Fig. 1, the recombination of methyl radicals takes place in gas phase as reported by many authors [20–24]. The fact that we did not detect C_2 products in the Knudsen diffusion regime supports this hypothesis. Figs. 4 and 5 show the time resolved pulse responses at 700 °C and Table 1 provides the quantitative evaluation by the zeroth moment of the pulse response (i.e. integrated area of the pulse) for both catalysts. The product responses except CO_2 are noisier than the reactant responses and were smoothened for better illustration in Figs. 4 and 5. The major differences in the reactivity of the two materials are the lower methane conversion and higher selectivity to ethane of $Mn/Na_2WO_4/SiO_2$ compared to those of magnesia. The carbon balance for the TAP measurements did not deviate more than 3%.

The positions of the peak maxima give evidence about the reaction sequence. In Fig. 4 one can clearly see that carbon monoxide is formed in parallel to the formation of ethane from methane. The origin of CO formation via a consecutive oxidation of methyl radicals is reasonable (Fig. 1). Methyl radicals are produced from methane at the catalyst surface by direct interaction with surface adsorbed oxygen [16]. They can be oxidized before desorption or by re-adsorption at the catalyst or quartz surface; if not they combine to ethane in the gas phase. The delayed peak maxima observed for magnesia compared to those of $Mn/Na_2WO_4/SiO_2$ indicate more

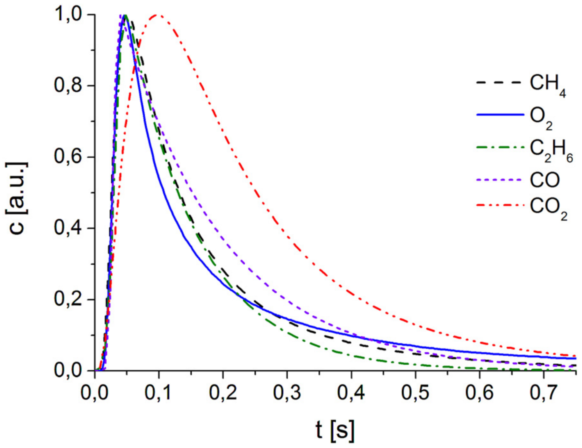

Fig. 5. TAP response of $CH_4/O_2/Ne$ 4/1/2 at $Mn/Na_2WO_4/SiO_2$ at 700 °C.

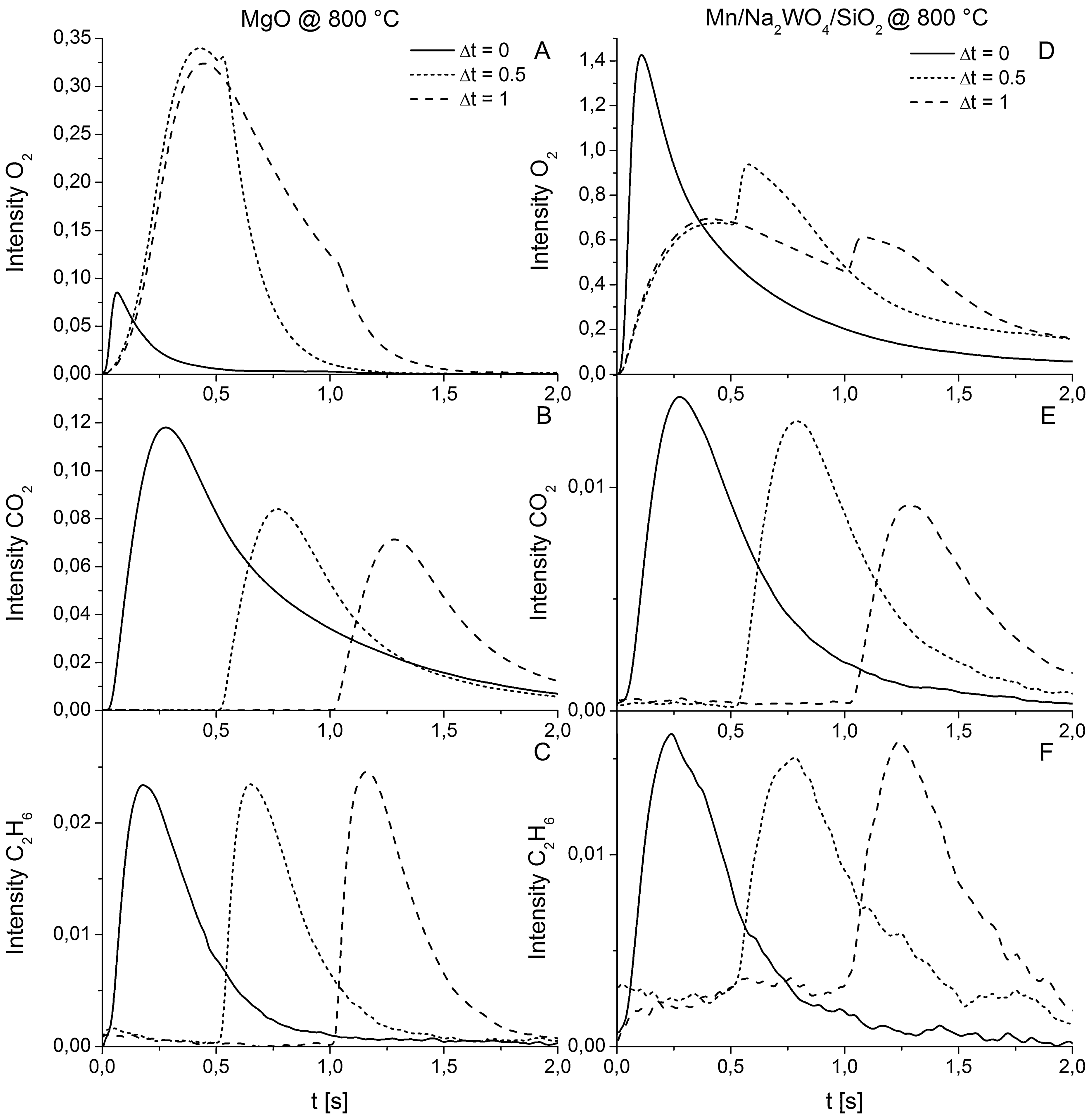

Fig. 6. TAP responses of sequential pulsing of first oxygen and then methane with a delay Δ*t* at 800 °C.

stable surface intermediates over magnesia, easing the consecutive oxidation of methyl radicals, which could be the major reason for the inferior selectivity to C_2 products (Table 1). For magnesia the response time of carbon dioxide is strongly delayed, indicating that it is produced by species strongly adsorbed onto magnesia or simply carbon dioxide interacts strongly with the catalyst surface. Analogous behavior can be observed when using ethane or ethylene as feed gas (not shown). No conversion could be observed by pulsing mixtures of hydrocarbon (methane, ethane or ethene) and oxygen in a reactor only filled with quartz particles. Therefore a gas phase activation of these components can be excluded. Interestingly, the oxygen balance cannot be closed for $Mn/Na_2WO_4/SiO_2$. Pulse experiments with pure oxygen result in a loss of oxygen, which can be explained by the oxidation of the material partially reduced under the TAP vacuum conditions.

Furthermore, sequential pulse experiments were used to investigate the reactivity of adsorbed oxygen at 800 °C. First oxygen is pulsed and next a pulse of methane is given with an offset of 0.0, 0.5 and 1 s. The oxygen response for magnesia is presented in Fig. 6A. The response of the oxygen pulse has a similar shape with an abrupt decay shortly after the pulse of methane. This rapid oxygen consumption is attributed to weakly adsorbed but highly reactive oxygen species. Due to decreasing concentration of these species with time, a decrease of the reaction products with increasing the delay of the methane pulse is expected to be observed. Carbon dioxide is identified as product showing the expected behavior (Fig. 6B). In contrast, in Fig. 6C the pulse intensity of ethane is not decreasing by delayed methane pulses. This indicates that the presence of a second species of more strongly adsorbed oxygen is responsible for the methyl radical formation. It should be mentioned that no

Table 1
Reactivity data of the two catalysts determined from TAP data at 700 °C.

Catalyst	Conversion CH_4 (%)	*S*CO (%)	*S*CO_2 (%)	*S*C_2H_6 (%)	*S*C_2H_4 (%)
$Mn/Na_2WO_4/SiO_2$	~2	3.6	1.4	95	0
MgO	16.0	83.4	14.6	2	0

Table 2
Integrated MS responses of the components presented in Fig. 6.

Catalyst Δt [s]	MgO			Mn/Na_2WO_4/SiO_2		
	O_2	CO_2	C_2H_6	O_2	CO_2	C_2H_6
0	2.15E – 2	8.93E – 2	1.15E – 2	7.83E – 1	8.59E – 3	1.33E – 2
0.5	1.58E – 1	5.28E – 2	1.16E – 2	1.15	8.23E – 3	1.28E – 2
1	2.23E – 1	4.50E – 2	1.16E – 2	1.21	6.77E – 3	1.38E – 2

product formation occurs by pulsing first methane and then oxygen.

The oxygen response for Mn/Na_2WO_4/SiO_2 is shown in Fig. 6D. When the two pulses are made at the same time the total pulse size is bigger, farther from Knudsen diffusion regime, and convective flow is more important, rendering the responses narrower. Immediately after methane enters the reactor, the oxygen response passes through a small maximum, which is not followed by an abrupt decay. The small maximum is an artifact resulting from the pulsing of methane and is also visible in the inert gas response (not shown). The missing fast decay is attributed to the lack of highly reactive adsorbed oxygen species as observed for MgO. The integrated quantities of the sequential pulse experiments are presented in Table 2. Due to the different methane to oxygen ratios the obtained quantities are not directly comparable with the simultaneous pulse experiments.

Nevertheless, Mn/Na_2WO_4/SiO_2 shows a similar response to that of magnesia at varying delay of methane pulse for carbon dioxide and ethane as presented in Fig. 6E and F, revealing the presence of a second species of more strongly adsorbed oxygen. Therefore it is reasonable that the ratio between strong and weak adsorbed oxygen species is responsible for the overall much higher C_2 selectivity of Mn/Na_2WO_4/SiO_2 compared to that of magnesia. Simultaneous pulsing of methane and $^{18}O_2$ was also examined to get closer insight into the nature of the oxygen species responsible for methyl radical formation. Unfortunately, no ^{18}O containing products were detected unless a very large amount of $^{18}O_2$ was used. Interestingly, the response at amu 36 is almost replaced by responses at the amu's 32 and 34 indicating a very fast exchange between gas phase, adsorbed and lattice oxygen.

Determination of apparent activation energies requires a constant amount of active sites within the studied temperature range. Due to the reduction of Mn/Na_2WO_4/SiO_2 in vacuum, that is temperature dependent, a constant amount of active sites is not provided. A reduction of magnesia in vacuum was not experimentally observed. Therefore the temperature dependence of the surface reactions of methane and the desired intermediates can only be provided for magnesia. Rate constants were determined by the zeroth moment of the reactant response assuming a first order rate expression of the hydrocarbon (methane, ethane or ethene) and oxygen [19]. Therefore, apparent activation energies could be determined from the Arrhenius plot in Fig. 7, as presented in Table 3. A loss of active sites by agglomeration was not observed. Interestingly, the apparent activation energies of methane and ethane are the same within the experimental error. The ratio between the pre-exponential factors of ethane to methane is 1.5, which is in accordance with the ratio of C–H bond quantity. Buyevskaya et al. found a significant difference between methane with 70 kJ/mol and ethane with 29 kJ/mol for samarium oxide, which was assigned to the different strength of the C–H bonds involved in the rate limiting step [16]. A similar value for the apparent activation energies of methane and ethane could be caused by the conditions, i.e. the bond cleavage is not the controlling parameter.

Table 3
Kinetic data of magnesia in the TAP reactor.

	CH_4	C_2H_6	C_2H_4
$E_{a,app}$ [kJ/mol]	113 ± 2	115 ± 6	82 ± 3
k_∞ [mol/l/s]	2.27E + 07	3.40E + 07	1.18E + 06

From the kinetic data it is now possible to estimate the maximum yield which would be achievable assuming that methane, ethane and ethene are only activated by surface catalyzed reaction pathways and each C–H activation successfully leads to the formation of the desired product. We used a simplified reaction network of consecutive reactions assuming a constant oxygen partial pressure as shown below and simulated it by application of a batch reactor model

$$2CH_4 \xrightarrow{O_2} C_2H_6 \xrightarrow{O_2} C_2H_4 \xrightarrow{O_2} 2CO_x$$

Fig. 8 shows the maximum yield of C_2 components as a function of the methane conversion at 750 °C. The maximum yield of C_2 is around 60%, at a methane conversion of 75%. Additionally, we simulated the C_2 yield at atmospheric conditions and constant oxygen partial pressure including gas phase reactions by application of a

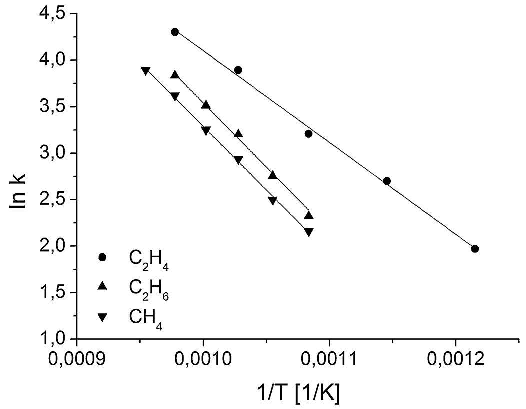

Fig. 7. Arrhenius plot of different substrates from TAP experiments with magnesia.

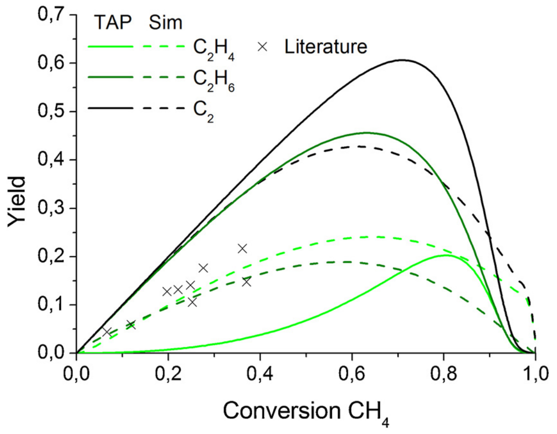

Fig. 8. Simulated yields of C_2 products as a function of methane conversion for magnesia calculated using the kinetic parameters obtained from the TAP measurements (solid line), the micro kinetic model of Sun/Marin [14] (dotted line), in comparison to the reported C_2 yield from literature [26–29] (cross symbol).

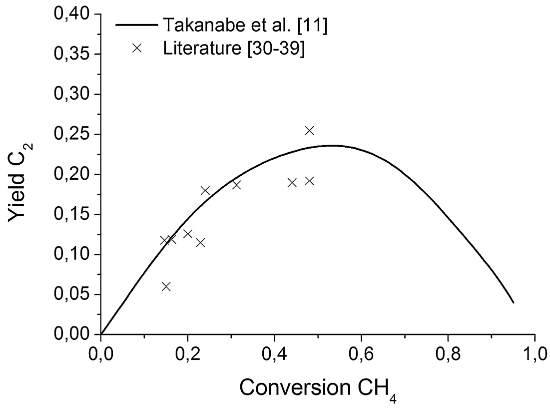

Fig. 9. Simulated yields of C_2 products as a function of methane conversion for $Mn/Na_2WO_4/SiO_2$ calculated using the kinetic parameters obtained from the OCM reaction in a recirculating batch reactor [11] (solid line) in comparison to singular reported C_2 yields from literature [30–39] (cross symbol).

batch reactor model as predicted by the model of Sun and Marin, which is the only available microkinetic model for magnesia based catalysts [14]. The maximum C_2 yield is predicted to be around 42% at a methane conversion of 60%. A comparison with the experimental data of other research groups with this model leads to a good prediction of the methane conversion, but a large overestimation of the C_2 selectivity [25].

Takanabe et al. [11] simulated the C_2 yield dependent of the methane conversion (Fig. 9) for $Mn/Na_2WO_4/SiO_2$ in a recirculating batch reactor at atmospheric pressure including direct oxidation pathways form methane and ethane to carbon oxides. The maximum C_2 yield is located around 24% at a methane conversion of 55%. Comparison of the simulated C_2 yield with those available in literature using various reactor setups and reaction conditions exhibits a conspicuous consistency. It is reasonable that suppression of unselective gas phase activation of methane, ethane and ethene will lead to notable higher C_2 yields as already shown for magnesia.

Independent of the type of reactors, different kinetic models used (TAP or normal pressurized reactor), and the type of catalysts, a methane conversion between 55% and 75% seems to be optimal to maximize the C_2 yield. Due to the explosion limit of methane/oxygen mixtures and the suppression of undesired gas phase reactions, the oxygen partial pressure must be kept at a low level. Therefore, a distributed oxygen feed along the reactor would be a good alternative which could be implemented by means of a membrane or stage-type reactor. Additionally, the formation of hot spots by the strongly exothermic total oxidation reaction has to be prevented.

From this qualitative insight into the reaction mechanism and the thermodynamical data some indication for the reaction engineering and reactor design can be drawn. The complexity of the reaction mechanism prevents accurate simulations of the derived reactor concepts. Therefore these have to be tested and investigated in detail before further upscaling.

3.4. *Thermodynamics and reaction engineering aspects*

Industrial application of heterogeneous catalyzed gas phase reactions are often realized in tubular reactors. In the case of exothermic reactions the heat production can lead to hot spot formations and in the worst case to a thermal runaway of the reactor. The critical tube diameter is a safety-related parameter giving the upper limit to assure the necessary heat transfer. The thermodynamic data from the NIST database [40] are used to calculate the reaction parameters. The enthalpy of reaction for the OCM in the temperature range of 500 to 1000 °C is −176 kJ/mol with an equilibrium constant of 1.01E+06. Therefore, OCM is highly exothermic and not thermodynamically limited in practice. The heat capacity of the gas mixture was calculated with Eq. (1).

$$C_p = x_{0,CH_4} C_{p,CH_4} + x_{0,O_2} C_{p,O_2} \tag{1}$$

For a mixture of 5% oxygen and 95% methane the heat capacity is 71.81 J/(mol K). The adiabatic temperature increase is 507 K under the assumption of a selectivity of 70% ethene and 30% to total combustion products and is calculated with Eq. (2).

$$\Delta T_{ad} = \frac{-\Delta H_R c_{A,0}}{\nu_A \rho \bar{c}_p} \tag{2}$$

To estimate the critical tube diameter of the fixed bed reactor Eqs. (3) and (4) from [41,42] are used.

$$d_{crit} = \frac{8\, Ge\, L\, R\, T_w^2}{Da\, E_a \Delta T_{Ad}} \tag{3}$$

$$Ge = \frac{0.125 d_p/d}{2 - \left(1 - 2d_p/d\right)^2} \tag{4}$$

In Eq. (3) the Damköhler number (*Da*) was added under the assumption of a first order reaction, caused by a quasi stationary methane concentration. The geometry factor (*Ge*) describes the volume properties of particles in a tube. Typical dimensions of tubular reactors are given by the length/diameter ratio of 100 and a particle size ratio to tube diameter of 0.1. With a wall temperature of 700 °C the critical tube diameter is 8 mm.

An increase of the oxygen mole fraction to 0.15 leads to a reduction of the critical tube diameter to 2 mm. Taking into account that upscaling leads to similar problems, the fixed bed reactor is unsuitable for OCM reactions at industrial conditions. The reason is the fast heat production and the low thermal conductivity of the catalyst bed. The absolute value of the critical tube diameter is dominated by the product distribution. Side reactions resulting in the formation of carbon monoxide and hydrogen will shift it to slightly higher values. Consecutive reactions resulting in the formation of carbon dioxide and water will shift it to lower values.

4. Conclusion

The experiments at elevated pressures point out that the yield of C_{2+} components increases with increasing pressure at the same residence time. Without a catalyst the yield is passing through a maximum, which is caused by the consecutive oxidation of C_{2+}. This occurs in homogenous gas phase reaction as well as heterogeneously catalyzed surface reaction at the catalyst itself, the reactor wall, and quartz packing. It is evident that the unselective gas phase reactions are more accelerated by higher pressures than surface catalyzed reactions. Thus it is reasonable that each specific reactor setup will pass through a maximum yield of C_{2+} components with increasing pressure. The methane conversions to maximize the C_2 yield are mostly in the 60–75% range. Sufficient oxygen has to be provided at a constant, but relatively low oxygen partial pressure. Kinetic models for OCM are developed for plug flow reactors with a relatively high oxygen feed fraction. Therefore for reactor simulations it is necessary to extrapolate these models to low fractions of oxygen leading to inaccuracies in the prediction of conversion and selectivity. Nevertheless, it is not possible to prevent the formation of hotspots inside the catalyst bed, due to the strongly exothermic total combustion. Jašo et al. [30] showed that the use of a fluidized bed reactor can overcome this flaw by providing isothermal conditions even at high oxygen to methane ratios. On the other hand, the broad residence time distribution of the gas will favor consecutive reactions, which are lowering the C_2 yield. Additionally, the physical strain could destroy the catalyst material during fluidization, but this was not observed in the case of $Mn/Na_2WO_4/SiO_2$. Another potential approach was done by Carr et al. by using a simulated countercurrent moving-bed chromatographic reactor to prevent total oxidation products by continuous separation of the reaction products [43]. C_2 yields of more than 50% were obtained [44,45].

Concerning the different strength of the C–H bonds between methane and ethane one could expect a lower activation energy for ethane, which is obviously negative for the C_2 yield. Interestingly magnesia does not show this behavior indicating a subsequent higher activation barrier to overcome, which could be related to the hydroxyl formation on the catalyst surface due to the C–H bond activation. Even though $Mn/Na_2WO_4/SiO_2$ was not suited for the determination of apparent activation energies at vacuum conditions due to vacuum-induced surface reduction, it was possible to find some significant differences between this catalyst and magnesia, explaining the higher C_{2+} selectivity observed for $Mn/Na_2WO_4/SiO_2$. Oxidation to carbon oxides proceeds over magnesia and $Mn/Na_2WO_4/SiO_2$ mainly by reaction of weakly adsorbed oxygen. The formation of methyl radicals proceeds by a second more strongly adsorbed oxygen species. $Mn/Na_2WO_4/SiO_2$ provides a much higher ratio of strongly adsorbed oxygen to weakly adsorbed oxygen, which highly improves the selectivity to C_2. Also, very fast oxygen exchange between adsorbed and lattice oxygen was observed for both materials, but at present it was not possible to assign the methyl radical formation to a specific type of oxygen such as lattice or strongly adsorbed oxygen by studies using labeled oxygen. There are still open questions about the nature of the oxygen species responsible for the methyl radical formation and the rate and selectivity determination step. Nevertheless qualitative suggestions for the reactor design and operation can be drawn.

Acknowledgment

We thank the Deutsche Forschungsgemeinschaft for financial support of our work in the cluster of excellence UniCat Berlin.

References

[1] J. Lunsford, Catal. Today 63 (2000) 165–174.
[2] S. Arndt, T. Otremba, U. Simon, M. Yildiz, H. Schubert, R. Schomäcker, Appl. Catal., A 425–426 (2012) 53–61.
[3] X.P. Fang, S.B. Li, J.Z. Lin, Y.L. Chu, J. Mol. Catal. 6 (1992) 427–433.
[4] U. Simon, O. Görke, A. Berthold, S. Arndt, R. Schomäcker, H. Schubert, Chem. Eng. J. 168 (2011) 1352–1359.
[5] S. Pak, P. Qiu, J. Lunsford, J. Catal. 230 (1998) 222–230.
[6] H. Liu, X. Wang, D. Yang, R. Gao, J. Nat. Gas Chem. 17 (2008) 59–63.
[7] P.F. Nelson, N.W. Cant, J. Phys. Chem. 94 (1990) 3756–3761.
[8] E. Morales, J. Lunsford, J. Catal. 5 (1989).
[9] J. Roos, S. Korf, R. Veehof, Appl. Catal., A 52 (1989) 147–156.
[10] J.T. Gleaves, G.S. Yablonskii, P. Phanawadee, Y. Schuurman, Appl. Catal., A 160 (1997) 55–88.
[11] K. Takanabe, E. Iglesia, J. Phys. Chem. C 113 (2009) 10131–10145.
[12] H. Zanthoff, M. Baerns, Ind. Eng. Chem. Res. (1990) 2–10.
[13] O. Korup, S. Mavlyankariev, M. Geske, C.F. Goldsmith, R. Horn, Chem. Eng. Process. 50 (2011) 998–1009.
[14] J. Sun, J. Thybaut, G. Marin, Catal. Today 137 (2008) 90–102.
[15] Q. Chen, P.M. Couwenberg, G.B. Marin, AIChE J. 40 (1994) 521–535.
[16] O.V. Buyevskaya, M. Rothaemel, H.W. Zanthoff, M. Baerns, J. Catal. 146 (1994) 346–357.
[17] E. Kondratenko, O. Buyevskaya, M. Soick, M. Baerns, Catal. Lett. 63 (1999) 153–159.
[18] G. Yablonskii, S. Shekhtman, Ind. Eng. Chem. Res. 5885 (1998) 2193–2202.
[19] J.T. Gleaves, G. Yablonsky, X. Zheng, R. Fushimi, P.L. Mills, J. Mol. Catal. A: Chem. 315 (2010) 108–134.
[20] T. Ito, J. Wang, C. Lin, J. Lunsford, J. Am. Chem. Soc. (1985) 5062–5068.
[21] D. Driscoll, J. Lunsford, J. Phys. Chem. (1985) 4415–4418.
[22] K.D. Campbell, E. Morales, J.H. Lunsford, J. Am. Chem. Soc. 109 (1987) 7900–7901.
[23] K. Campbell, J. Lunsford, J. Phys. Chem. 92 (1988) 5792–5796.
[24] E. Mallens, J. Hoebink, G. Marin, J. Catal. 234 (1996) 222–234.
[25] S. Arndt, G. Laugel, S. Levchenko, R. Horn, M. Baerns, M. Scheffler, R. Schlögl, R. Schomäcker, Catal. Rev. 53 (2011) 424–514.
[26] J.S.J. Hargreaves, G.J. Hutchings, R.W. Joyner, C.J. Kiely, Catal. Today 10 (1991) 259–266.
[27] C. Chevalier, P.R. de la Piscina, M. Ceruso, A. Choplin, J.M. Basset, Catal. Today 4 (1989) 433–439.
[28] V. Choudhary, J. Chem. Technol. Biotechnol. 68 (1997) 177–186.
[29] V. Choudhary, S. Mulla, J. Chem. Soc., Faraday Trans. 75 (2000) 828–834.
[30] S. Jašo, S. Sadjadi, H. Godini, U. Simon, S. Arndt, O. Görke, A. Berthold, H. Arellano-Garcia, H. Schubert, R. Schomäcker, G. Wozny, J. Nat. Gas Chem. 21 (2012) 534–543.
[31] K. Takanabe, E. Iglesia, Angew. Chem. Int. Ed. 47 (2008) 7689–7693.
[32] A. Malekzadeh, M. Abedini, A. Khodadadi, Catal. Lett. 84 (2002) 45–51.
[33] A. Palermo, J. Vazquez, R. Lambert, Catal. Lett. 68 (2000) 191–196.
[34] A. Malekzadeh, A. Khodadadi, J. Nat. Gas Chem. 16 (2007) 121–129.
[35] S. Ren, S. Qin, J. Zhu, X. Peng, C. Hu, Ind. Eng. Chem. Res. (2010) 2078–2083.
[36] L. Chou, Y. Cai, B. Zhang, J. Niu, J. Nat. Gas Chem. 11 (2002) 131–136.
[37] S.M.K. Shahri, A.N. Pour, J. Nat. Gas Chem. 19 (2010) 47–53.
[38] A. Karimi, R. Ahmadi, H. Zadeh, Pet. Coal (2007) 2–6.
[39] H. Bozorgzadeh, R. Ahmadi, Pet. Coal 53 (2011) 84–90.
[40] U.S. Secretary of Commerce, http://webbook.nist.gov/chemistry/ (2011).
[41] D.A. Frank-Kamenetskii, Diffusion and Heat Transfer in Chemical Kinetics, second ed., Plenum Press, London, New York, 1969.
[42] E.U. Schlünder, Chem. Ing. Tech. 38 (1966) 967–979.
[43] M.C. Bjorklund, R.W. Carr, Catal. Today 25 (1995) 159–168.
[44] A.L.Y. Tonkovich, R.W. Carr, R. Aris, Science 262 (1993) 221–223.
[45] A.L.Y. Tonkovich, R.W. Carr, Chem. Eng. Sci. 49 (1994) 4647–4656.